

Experiments with Fluid Friction in Roughened Pipes

BY C. F. COLEBROOK AND C. M. WHITE

Imperial College, London

(Communicated by G. I. Taylor, F.R.S.—Received 15 February 1937)

Nikuradse (1933; Prandtl 1933), experimenting with pipes roughened internally by a uniform layer of sand, found that such pipes were indistinguishable from perfectly smooth ones, provided that the pressure gradient was less than that given by

$$\frac{\rho V_* k}{\mu} = 4,$$

where $V_* = \sqrt{(\tau_0/\rho)}$, τ_0 = shear stress at wall, ρ = density of fluid, μ = viscosity of fluid, k = diameter of roughness grains. With lesser flows neither the resistance nor the distribution of velocity was measurably influenced by the size of the roughness grains, and the observed resistance law was satisfactorily of the type required by the Kármán-Prandtl theory for smooth surfaces. This law is usually expressed in the following form:

$$\frac{1}{\sqrt{\lambda}} = 2 \log \frac{\rho U d}{\mu} \sqrt{\lambda} - 0.8, \quad (1)$$

where λ is the coefficient of friction in the formula $h = \lambda \frac{lU^2}{2gd}$, and U = mean velocity, d = pipe diameter, and the "2" and the "0.8" are experimentally determined coefficients relating to turbulence and boundary conditions respectively.

Rewriting (1) to express the resistance coefficient $\frac{\tau_0}{\rho U^2}$ as a function of the Reynolds Number $\frac{\rho V_* d}{\mu}$, we get

$$\frac{\tau_0}{\rho U^2} = \frac{1}{8} \left(2 \log 1.13 \frac{\rho V_* d}{\mu} \right)^{-2}. \quad (2)$$

With much greater pressure gradients, Nikuradse found that fully rough conditions had developed provided

$$\frac{\rho V_* k}{\mu} > 60,$$

and the friction coefficient $\tau_0/\rho U^2$ was then constant for any one pipe with any given surface. The type of law required by the theory was found, viz.

$$\frac{\tau_0}{\rho U^2} = \frac{1}{8} \left(2 \log \frac{3.7d}{k} \right)^{-2}, \quad (3)$$

in which the resistance is seen to be independent of viscosity which is in effect replaced by grain size k .

Thus a pipe may be regarded as perfectly smooth when $\frac{\rho V_* k}{\mu}$ is less than 4, or completely rough when $\frac{\rho V_* k}{\mu}$ exceeds 60, and the appropriate resistance laws are given by (2) and (3) respectively. Between these values, however, i.e. within the range

$$4 < \frac{\rho V_* k}{\mu} < 60,$$

flow in Nikuradse's pipes is in a transitional state in which both viscosity and grain size influence the resistance. In this transition range the resistance law is necessarily more complicated since both μ and k are involved.

The two simpler particular cases (2) and (3), when generalized as

$$\frac{\tau_0}{\rho U^2} = \frac{1}{8} \left(2 \log \frac{0.113d}{y_1} \right)^{-2}, \quad (4)$$

are seen as the result of integrating the equation

$$\frac{du}{dy} = \frac{2.5}{y} \sqrt{\frac{\tau_0}{\rho}}$$

between the limits $y = y_1, \quad u = 0,$

and $y = 0.225r, \dagger \quad u = U.$

Here the lower limit y_1 is the distance from the wall of an arbitrarily selected point where the velocity is assumed zero. In equation (3) the lower limit conforms with the experimental value

$$y_1 = \frac{1}{33}k,$$

the velocity being taken as zero at a distance y_1 equal to 1/33 of the grain diameter, measured from the centre line of the grains inwards towards the

† The numerical factor 0.225 can be obtained by a simple integration across the pipe and is practically independent of y_1/r when this is small. r = radius, $d/2$.

centre of the pipe. Similarly in eqn. (2) the lower limit measured in the same manner is

$$y_1 = 0.1 \frac{\mu}{\rho V_*} \cdot \dagger$$

Within the transition range this lower limit, y_1 , varies gradually between the values mentioned, and can be expressed in the form

$$\frac{\rho V_* y_1}{\mu} = \phi_1 \left(\frac{\rho V_* k}{\mu} \right),$$

which conveniently separates the variables y_1 and k . Prandtl, however, adopts the alternative form

$$\sqrt{\frac{\rho U^2}{8\tau_0}} - 2 \log \frac{r}{k} = \phi \left(\frac{\rho V_* k}{\mu} \right), \tag{4a}$$

which by virtue of (4), which converts the left-hand side to $2 \log \frac{0.225k}{y_1}$, is disclosed as

$$\frac{y_1}{k} = \phi_2 \left(\frac{\rho V_* k}{\mu} \right).$$

These functions relating to conditions in the immediate vicinity of the wall can only be found satisfactorily by experiment.

Nikuradse's experimental results are represented by the full lines in fig. 1 in which $\frac{8\tau_0}{\rho U^2}$ (i.e. λ) is plotted logarithmically against $\frac{\rho U d}{\mu}$.

To the right, each pipe has a constant coefficient indicating that completely rough conditions have been reached, whereas to the left all curves converge towards that for smooth surfaces. It appears that transition between smooth and rough is always completed within the area shown shaded in fig. 1.

The manner in which each curve leaves the smooth law curve depends very much upon the type of roughness. The full-line curves in fig. 1 were obtained by Nikuradse for sand-roughened surfaces, but other surfaces give results which are more of the type shown by curve *B*, which is for a 2 in. galvanized pipe tested by Heywood (1924). Curve *C* for a 5 in. new wrought iron pipe‡ is similar and has been selected as typical of this surface. At the

† The values 1/33 and 0.1 are consistent with Nikuradse's final resistance results, but differ slightly from the values he mentions as found from velocity distributions, the differences being less than the uncertainty of measurement of the latter.

‡ J. R. Freeman as quoted by Mills (1923).

highest speeds both B and C seem to approach square law resistance and it is possible with some certainty to assign definite values of r/k to these pipes, using Nikuradse's constants as providing a basic standard of roughness.

The data of fig. 1 become greatly simplified when plotted in fig. 2 in which the ordinate is the left-hand side of equation (4a) plotted naturally, while the abscissa is $\frac{\rho V_* k}{\mu}$ plotted logarithmically. The smooth law appears as the sloping straight line to the left, and the square law as the horizontal line to the right. Nikuradse's results become a single curve which, by its form, indicates fairly rapid transition from one law to the other, but pipes B and C definitely involve another parameter and curve over far more gradually.

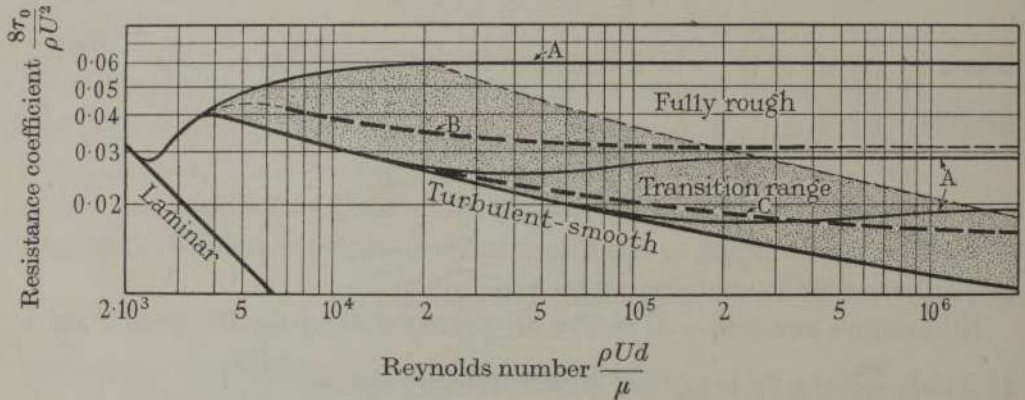


FIG. 1—Resistance to flow through pipes. Curves A are for Nikuradse's sand roughened pipes; B , Heywood 2 in. galvanized; and C , Freeman 5 in. wrought iron.

Possibly part of this difference is due to differences in geometrical form of the roughness protuberances, but the main cause is, no doubt, to be found in a variation in size of individual protuberances. It is reasonable to suppose that a grain only begins to contribute to the resistance when the local speeds are high enough to cause the grain to shed eddies. Until then its form drag is comparatively small and the tangential drag constitutes the major part of the resistance. The tangential drag is not greatly influenced by dimensions normal to the motion; so the unimportance of k at slow speeds is understandable. Nikuradse's curves may be interpreted as showing that a few grains shed eddies when $\frac{\rho V_* k}{\mu} = 4$; and on the average perhaps half the grains shed eddies when $\frac{\rho V_* k}{\mu}$ exceeds 10 approx.

To test this interpretation, experiments were made with sand grains falling in still water. Various sizes of grain were used and it was found that square law drag (to be associated with the shedding of eddies) occurred only when the grains exceeded 0.5 mm. in diameter. The falling speed was then 5 cm./sec. approximately, and when the drag stress was estimated by dividing half the effective weight of the grain by $\frac{\pi k^2}{4}$, a value of $\frac{\rho V_* k}{\mu} = 14$ was obtained, which is sufficiently near Nikuradse's value to support the argument.

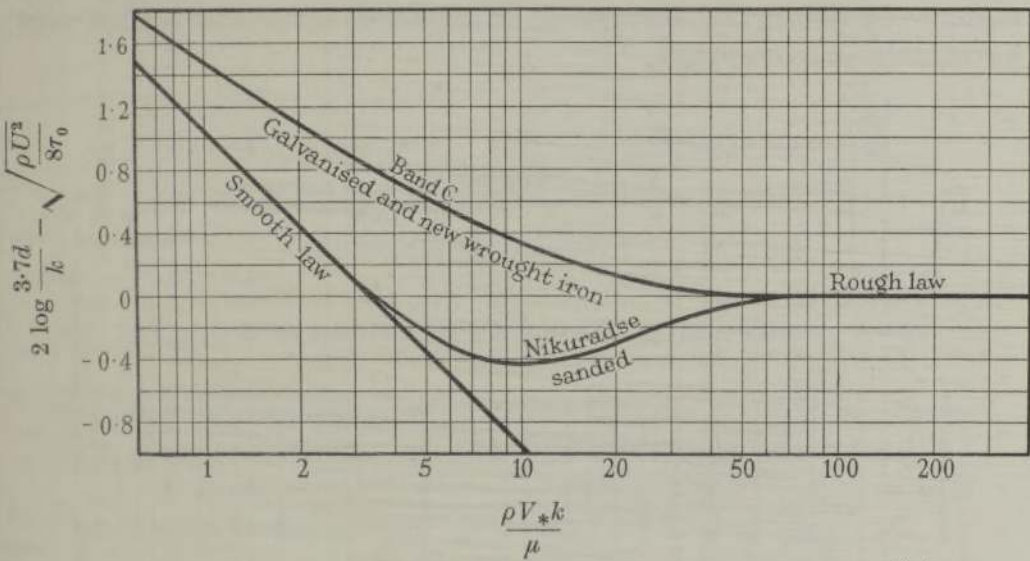


FIG. 2—Deviations from "rough" law resistance as a function of $\frac{\rho V_* k}{\mu}$.

With a roughness composed of grains of many different sizes the larger grains come into action at lower speeds than the smaller. Transition from smooth to rough should begin therefore at a speed determined by the size of the largest grains. One might expect also that transition would be complete at a speed determined by the smallest grains, but the experiments did not confirm this.

The main object of the present experiments was to determine how the nature of the roughness influenced the transition. The experiments were all made with the same pipe, 5.35 cm. diameter and approximately 6 m. long, using air. The pipe was split longitudinally in order to expose the inner surface to which the necessary sand grains were fixed by bituminous paint or by Chatterton's compound. The two halves were held together by metal straps and the joints made air-tight with adhesive tape. The whole was then

mounted and aligned as accurately as possible on a stiff joist, as shown in the general arrangement fig. 3.

The test length was approximately 50 diameters, separated from the ends of the pipe by about 12 diameters downstream and 50 diameters upstream. A greater test length would have been desirable but preliminary trials showed that the entrance effects extended downstream rather farther than had been anticipated. It was considered advisable, therefore, to insert a diffusing baffle near the inlet in order to ensure development of the ultimate velocity distribution before reaching the test length. Four inter-connected pressure holes were used at each section, but the errors of individual holes as shown by tests of each one against its neighbour at the same section were fortunately quite negligible.

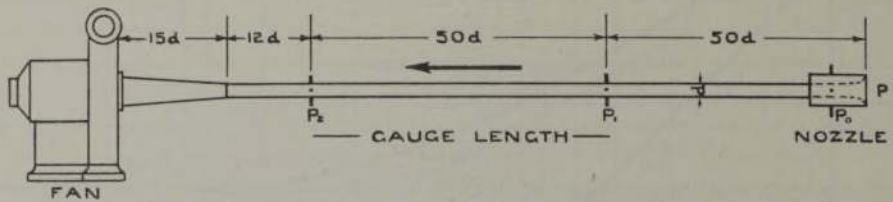


FIG. 3—General arrangement of test pipe, metering nozzle, and fan.

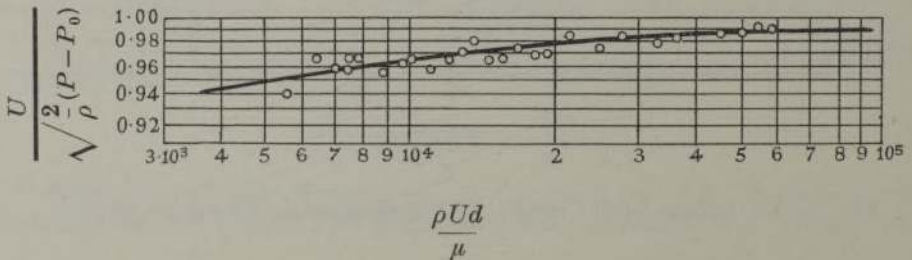


FIG. 4—Calibration curve for metering nozzle.

The air was metered by a nozzle to "V.D.I. Normalduse" upstream profile cast in paraffin wax and fitted to the pipe inlet. This nozzle was calibrated *in situ*, using the pipe in its smooth state as standard. The resulting calibration curve, fig. 4 is of quite usual type, and is probably correct within 1 %.

Six different types of roughness were formed from various combinations of two sizes of sand grain, viz. 0.035 cm. diam. and 0.35 cm. diam. As shown in fig. 5, the whole surface was roughened for some of the experiments, while for others part of the surface was left smooth. The fine grains lay in a very uniform manner just touching each other; and fig. 5a shows a typical large grain and its mounting. The six surfaces together fall into two systematic series: Nos. 0, I, II and III; and Nos. V, IV and III. In the first series the

area covered by large grains progressively increases; but in the second series, the large grains remain constant while the area covered by small grains increases.

The test results for the first series are shown together in fig. 6. Here surface 0 is represented by the smooth law

$$\frac{8\tau_0}{\rho U^2} = \left(2 \log 1.13 \frac{\rho V_* d}{\mu}\right)^{-2}, \tag{2}$$

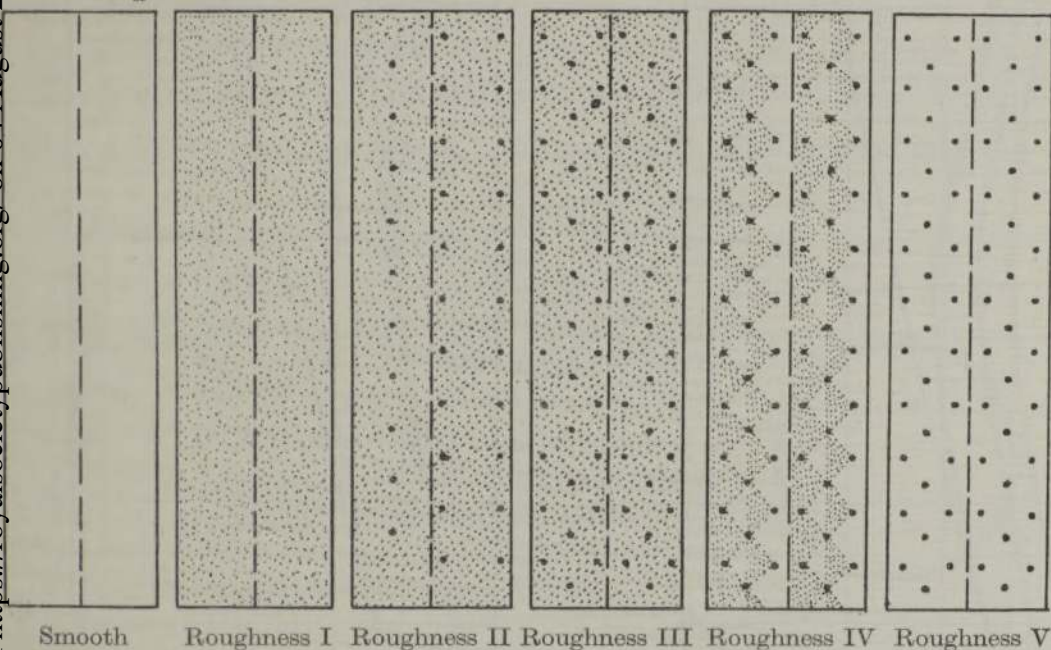
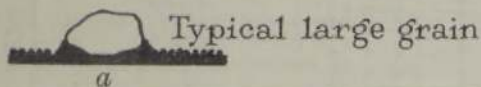


FIG. 5—Surfaces used in the experiments.

assumed for the nozzle calibration. Surface I, uniform fine sand, is indistinguishable from smooth when Re is of the order of 6000, but, as the speed increases, transition to rough law begins and is completed at $Re = 100,000$. The effect of the addition of a few large grains to this surface is clearly shown by tests with surface II. The resistance at high speeds is increased by approximately 12%, and this is the result of placing grains ten times the size of the fine sand on approximately 2% of the area. At low speeds the effect is more marked, the resistance being increased by 20% at $Re = 10,000$. Transition is seen to be very gradual, certainly including the whole of the turbulent range up to $Re = 100,000$. Surface III with twice as many large grains also shows these characteristics but in greater degree.

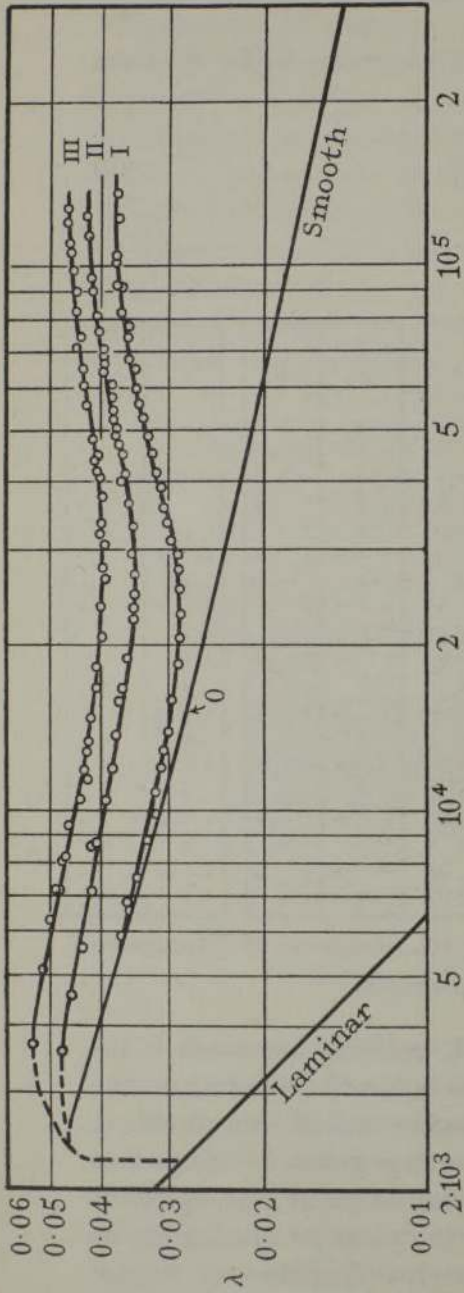
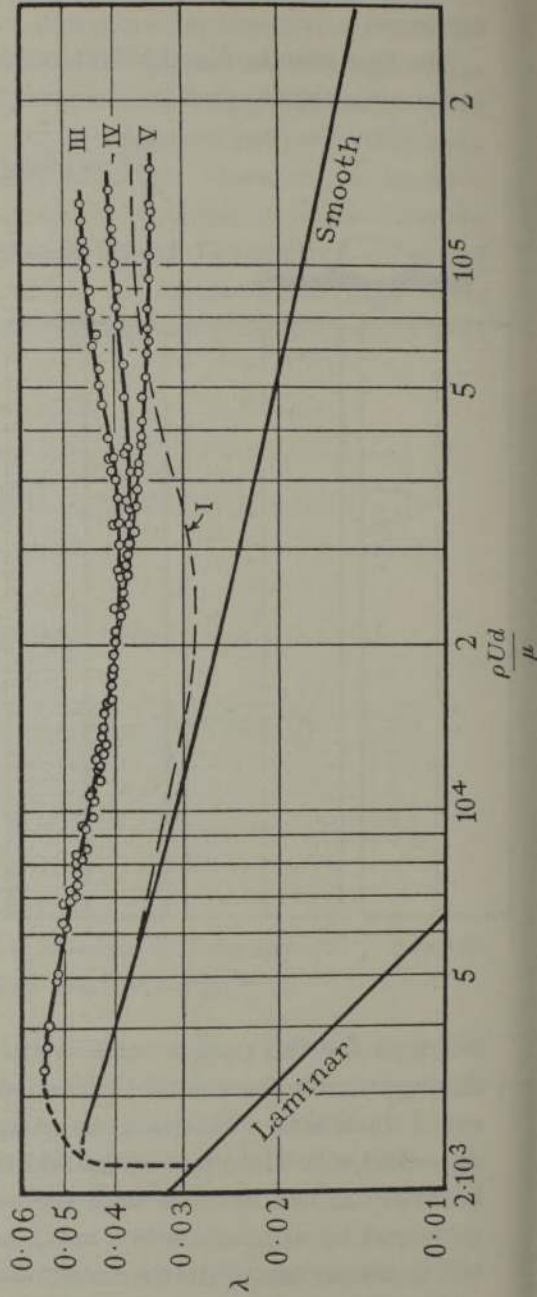


FIG. 6



It is interesting to note that the action of the fine grains, if judged by the rising part of the curves to the right of fig. 6, is, if anything, delayed by the presence of the larger grains, the just noticeable displacement of the upper curves in fig. 6 being to the right despite greater pressure gradients. No doubt this is due to some shielding effect.

In the second series of surfaces, in which the large grains were constant and the area of fine grains varied, the most interesting feature is that below $R = 20,000$ it is impossible to distinguish between the three surfaces, the test points lying perfectly upon a single curve as seen in fig. 7. The shielding effect of the larger grains is here clearly demonstrated by comparison with the uniform fine sand surface, the curve for which is shown dotted. The Reynolds number at which the fine grains are just detectable is more than three times greater when the large grains are present than when they are absent. This is with approximately the same value of $\frac{\tau_0}{\rho U^2}$, so the shielding effect is equally marked if expressed in terms of $\frac{\rho V_* k}{\mu}$.

That the rising part of the curve is linked with the action of the finer closely spaced grains, is clearly demonstrated by curve V of fig. 7. This is the only curve without the rise, and the surface to which it relates is the only one without appreciable area of closely spaced grains.

The latter surface, V, shows a rather unexpected constancy of coefficient at the highest speed. Judged by areas, 95 % of this pipe was smooth and likewise 80 % of the perimeter of the cross section, fig. 8. The wake from individual grains must spread out fanwise very rapidly, otherwise the lack of influence of viscosity over the 95 % of smooth area is inexplicable.

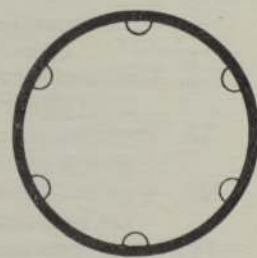


FIG. 8—Section of pipes Nos. III, IV and V.

There is, however, no reason to doubt the experiments; in fact the numerical values for $\frac{k_s}{k}$ at high speeds for surface V is in agreement with the recent work of Schlichting (1936) who, by another experimental method and using a surface studded with hemispherical rivet heads, obtained values from which fig. 9 is computed.

The square law values of λ for all five surfaces are given in Table I together with equivalent sand sizes, k_s , computed on Nikuradse's basis, i.e.

$$\frac{\tau_0}{\rho U^2} = \frac{1}{8} \left(2 \log \frac{3.7d}{k_s} \right)^{-2}$$

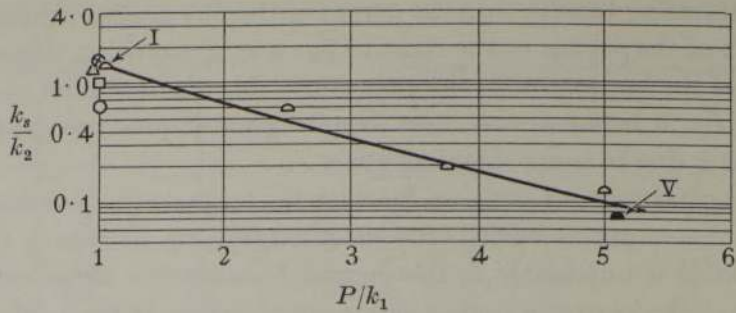


FIG. 9—Comparison of surfaces I and V with Schlichting's experiments. P = distance between protuberances; k_2 = measured size of protuberances normal to wall; k_s = size computed from observed resistance using Nikuradse's constants; k_1 = diameter of protuberance in plane of wall. \otimes Hamburg sand; \circ spheres; \circ cup-head rivets; \triangle surface I Aylesford sand; \square sand-Nikuradse; \blacktriangle sand grains—spaced—surface V.

TABLE I—RESISTANCE COEFFICIENTS FOR VARIOUS SURFACES AT HIGH SPEEDS, I.E. WHEN $\frac{\rho V_* k}{\mu}$ EXCEEDS 150

Description of surface	$\frac{8\tau}{\rho U^2}$	k_s cm.	$\frac{k_s}{k}$
I. Uniform sand 0.035 cm. diam. in 2 in. pipe	0.0369	0.048	1.36
II. Uniform sand with large 0.35 cm. grains covering $2\frac{1}{2}\%$ of area	0.0425	0.073	—
III. Uniform sand with large 0.35 cm. grains covering 5% of area	0.047	0.093	—
IV. 48% area smooth, 47% area uniformly covered fine grains, 5% area covered large grains	0.041	0.066	—
V. 95% area smooth, 5% area covered large grains	0.034	0.038	0.11
Hamburg sand $k = 0.135$ cm. tested by Schlichting	—	0.222	1.64
Cup-head rivets touching, 0.26 cm. rad. tested by Schlichting	—	0.365	1.40
Polished spheres touching, 0.41 cm. diam. tested by Schlichting	—	0.257	0.63
Cup-head rivets, 5 diam. apart, 0.26 cm. rad. tested by Schlichting	—	0.031	0.12

When the transition curves for surfaces I to V are expressed as a function of $\frac{\rho V_* k_s}{\mu}$ as in fig. 10, all are seen as a single systematic family of curves, each progressively showing less and less dip, together with earlier deviation

TABLE II

Roughness I

$$k_s = 0.048 \text{ cm.} \quad \frac{r}{k_s} = 55$$

$\frac{\rho U d}{\mu}$	$\lambda = \frac{8\tau}{\rho U^2}$	$\text{Log} \frac{\rho V_* k_s}{\mu}$	$2 \log \frac{3.7d}{k_s} - \frac{1}{\sqrt{\lambda}}$
5,900	0.0363	0.559	-0.03
7,510	0.0340	0.650	-0.20
10,700	0.0316	0.787	-0.41
16,050	0.0294	0.947	-0.61
22,800	0.0285	1.093	-0.70
36,000	0.0303	1.305	-0.53
53,000	0.0331	1.492	-0.28
67,700	0.0350	1.610	-0.13
91,500	0.0369	1.753	0
136,000	0.0369	1.925	0.02

Roughness II

$$k_s = 0.073 \text{ cm.} \quad \frac{r}{k_s} = 36.3$$

3,580	0.0471	0.578	0.25
5,580	0.0431	0.753	0.05
10,400	0.0388	1.000	-0.22
19,000	0.0353	1.241	-0.46
26,800	0.0344	1.385	-0.54
32,600	0.0344	1.470	-0.54
47,100	0.0366	1.642	-0.37
68,500	0.0395	1.822	-0.17
90,000	0.0411	1.949	-0.07
122,000	0.0425	2.088	0

Roughness III

$$k_s = 0.093 \text{ cm.} \quad \frac{r}{k_s} = 28.5$$

3,700	0.0534	0.725	0.305
5,070	0.0513	0.853	0.21
7,060	0.0475	0.980	0.05
11,800	0.0431	1.182	-0.19
18,300	0.0405	1.360	-0.34
26,700	0.0390	1.515	-0.44
40,500	0.0397	1.700	-0.39
55,700	0.0422	1.851	-0.245
82,600	0.0443	2.033	-0.12
127,500	0.0462	2.232	-0.02

TABLE II—(continued)

Roughness IV

$$k_s = 0.066 \text{ cm.} \quad \frac{r}{k_s} = 40.3$$

$\frac{\rho U d}{\mu}$	$\lambda = \frac{8\tau}{\rho U^2}$	$\text{Log} \frac{\rho V_* k_s}{\mu}$	$2 \log \frac{3.7d}{k_s} - \frac{1}{\sqrt{\lambda}}$
3,360	0.0545	0.538	0.67
4,880	0.0515	0.688	0.55
7,700	0.0467	0.864	0.32
15,650	0.0411	1.145	0.025
29,600	0.0379	1.403	-0.20
41,800	0.0373	1.550	-0.23
66,500	0.0381	1.756	-0.18
91,200	0.0345	1.902	-0.07
110,000	0.0402	1.987	-0.04
127,500	0.0408	2.053	0

Roughness V

$$k_s = 0.038 \text{ cm.} \quad \frac{r}{k_s} = 69.6$$

5,100	0.0514	0.470	1.01
7,400	0.0475	0.614	0.83
10,750	0.0445	0.762	0.69
19,300	0.0402	0.994	0.42
30,600	0.0374	1.178	0.25
42,000	0.0359	1.307	0.14
63,500	0.0349	1.480	0.06
83,000	0.0345	1.595	0.04
116,000	0.0340	1.736	-0.005
127,200	0.0341	1.775	-0.005

from the smooth law. Nikuradse's curve for uniform roughness, shown broken, is noticeably flatter than that for the present uniform surface I, due perhaps to the latter being more regular. Surface V, which is the other extreme, being smooth with large lumps, has a transition almost indistinguishable from that for galvanized iron pipes for which a typical curve is also shown in fig. 10.

The early part of transition is perhaps better shown as a function of $\frac{\rho V_* k_m}{\mu}$ as in fig. 11, which is similar to fig. 10 except that k_m , the maximum size of grain, is now used instead of k_s the equivalent Nikuradse size. Again a family of curves is obtained, but now all appear to radiate from a single origin on the smooth curve at $\frac{\rho V_* k_m}{\nu} = 5$ approx., lending some support to the view that it is the large grains which control the beginning of transition.

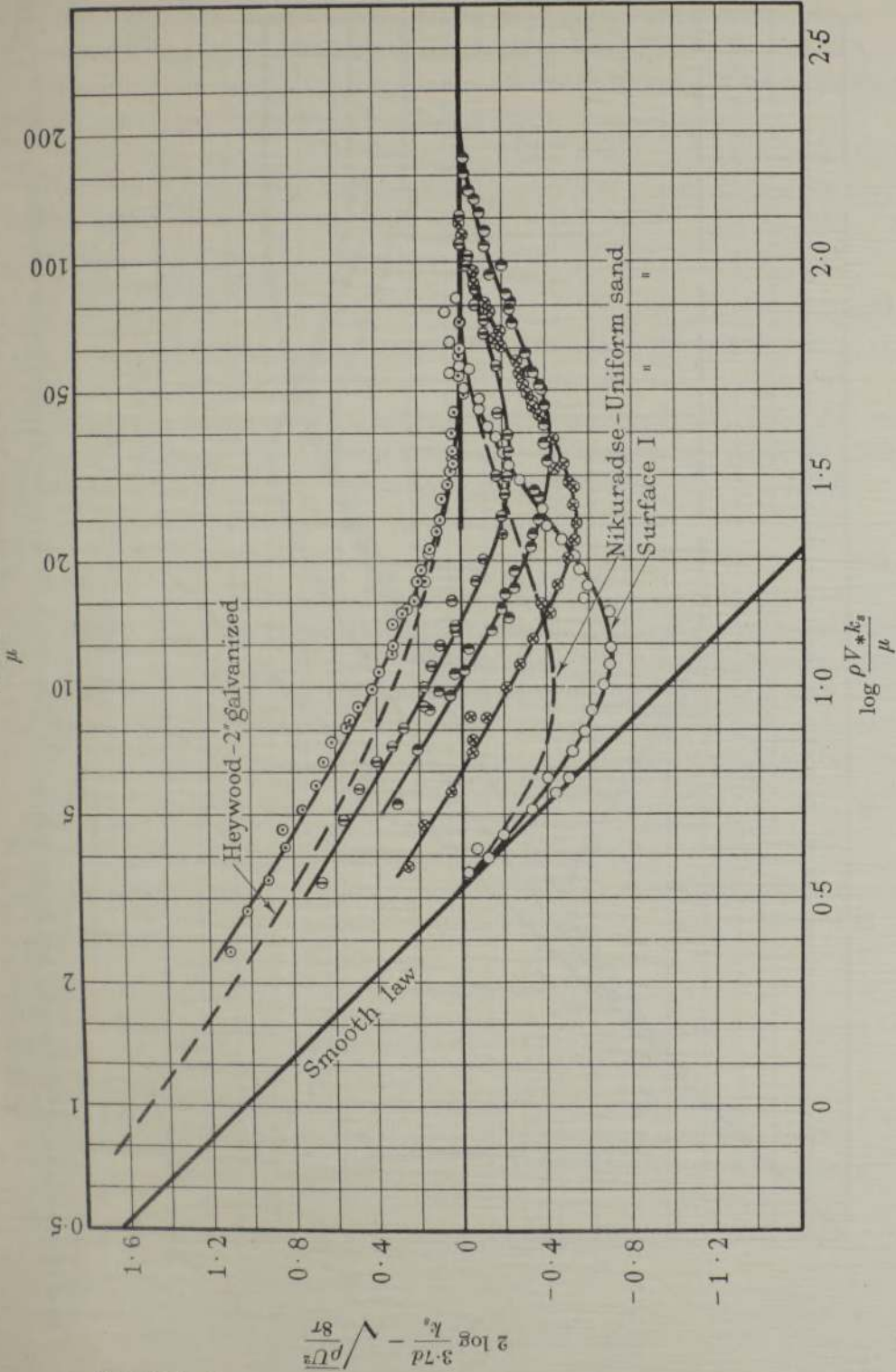


FIG. 10—Deviations from "rough" law as function of $\rho V_* k_s / \mu$, where k_s is equivalent grain size. The surfaces I to V are described in fig. 5 and in Table I. O surface I; \otimes surface II; \oplus surface III; \odot surface IV; \odot surface V.

Downloaded from https://royalsocietypublishing.org/ on 04 August 2022

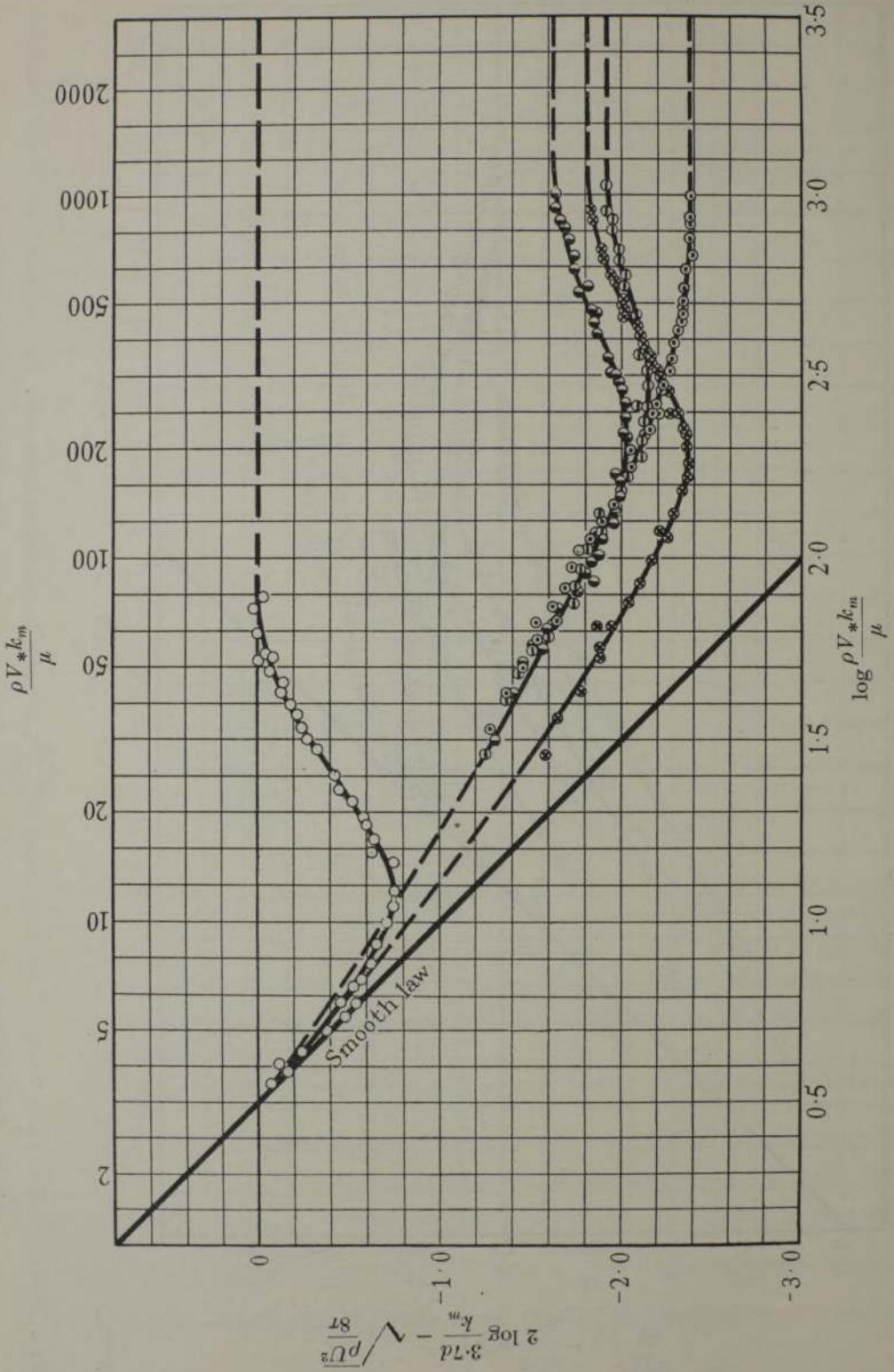


FIG. 11—Deviations from "rough" law as function of $\frac{\rho V_* k_m}{\mu}$, where k_m is diameter of largest grains. \circ surface I; \otimes surface II; \bullet surface III; \ominus surface IV; \odot surface V. (For descriptions see Table I and fig. 5.)

Accepting that transition begins at this value, the transition range for surface V is between six and seven times as long as that for the uniform surface I. Over much of this range the curve of resistance coefficient (fig. 7) runs nearly parallel to the smooth law.

Such characteristics have been previously mentioned by other workers (Hopf 1923), and it has been suggested, no doubt correctly in some cases, that the cause is "wall waviness" as distinct from surface roughness, but the present experiments show that such results may also be attributed to surface roughness when this is of non-uniform type.

Altogether more than 200 test points were obtained and all are included in the diagrams. Ten typical points for each surface are given in Table II.

The work was carried out in the Civil Engineering Dept. of the Imperial College of Science and Technology, and the authors are indebted to the Clothworkers' Company whose generosity made the research possible.

SUMMARY

Nikuradse, experimenting with flow through uniformly roughened pipes, found comparatively abrupt transition from "smooth" law at slow speeds to "rough" law at high speeds. Other experimenters using surfaces of the nature of cast iron, wrought iron or galvanized steel, have obtained results which can only be explained by a much more gradual transition between the two resistance laws. The present experiments show that with non-uniform roughness, transition is gradual, and in extreme cases so gradual that the whole working range lies within the transition zone. This closes the gap between Nikuradse's artificial roughnesses, and those normally found in pipes.

REFERENCES

- Heywood, F. 1924 *Min. Proc. Instn Civ. Engrs*, **219**, 174.
Hopf 1923 *Z. angew. Math. Mech.* **3**, No. 5, 329.
Mills 1923 "Flow of Water in Pipes." (U.S.A.)
Nikuradse, J. 1933 *Forschungsh. Ver. dtsh. Ing.* No. 361.
Prandtl, L. 1933 *Z. Ver. dtsh. Ing.* **77**, No. 5, 105.
Schlichting, H. 1936 *Werft, Reed. Hafen*, **8**, 99.